The American Journal of Pathology, Vol. 178, No. 5, May 2011

DOI: 10.1016/j.ajpath.2011.01.031

Immunopathology and Infectious Diseases

Human Proteins with Affinity for Dermatan Sulfate Have the Propensity to Become Autoantigens

Jung-hyun Rho,* Wei Zhang,*† Mandakolathur Murali,‡ Michael H.A. Roehrl,§ and Julia Y. Wang*

From the Department of Medicine, Channing Laboratory, Brigham and Women's Hospital, and the Department of Pathology,‡ Massachusetts General Hospital, Harvard Medical School, Boston, Massachusetts; the Department of Gastroenterology,† Guiyang Medical College, Guiyang, Guizhou, China; and Department of Pathology and Laboratory Medicine,§ Boston Medical Center, Boston University School of Medicine, Boston, Massachusetts*

The mystery of why and how a small, seemingly disparate subset of all self molecules become functional autoantigens holds a key to understanding autoimmune diseases. Here and in a companion article in this issue, we show that affinity of self molecules to the glycosaminoglycan dermatan sulfate (DS) is a common property of autoantigens and leads to a specific autoreactive B-1a cell response. Autoimmune ANA/ENA reference sera react preferentially with DS affinity-fractionated cellular proteins. Studying patients with autoimmune diseases, we discovered patient-specific complex autoantigen patterns that are far richer and more diverse than previously thought, indicating significant pathological heterogeneity even within traditionally defined clinical entities, such as systemic lupus erythematosus. By shotgun sequencing of DS affinity-enriched proteomes extracted from cell lines, we identified approximately 200 autoantigens, both novel and previously linked to autoimmunity, including several well-known families of autoantigens related to the nucleosome, ribonucleoproteins, the cytoskeleton, and heat shock proteins. Using electron microscopy, we recognized direct interaction with dead cells as an origin of autoantigenic association of DS with self molecules. DS affinity may be a unifying property of the human autoantigen-ome (ie, totality of self molecules that can serve as functional autoantingens) and thus provides a promising tool for discovery of autoantigens, molecular diagnosis of autoimmune diseases, and development of cause-specific therapies. *(Am J Pathol 2011, 178:2177–2190; DOI: 10.1016/j.ajpath.2011.01.031)*

Autoimmune diseases are among the most poorly understood medical conditions, although it is well accepted that they are caused by aberrant immune responses directed at endogenous molecules and tissues of the body. Autoimmune diseases encompass a wide spectrum of clinical presentations, and more than 80 types have been classified, based primarily on systemic or organ-specific involvement.[1] Common systemic autoimmune diseases include systemic lupus erythematosus (SLE), rheumatoid arthritis, and Sjögren syndrome; localized diseases include type 1 diabetes, multiple sclerosis, and Graves disease. Both precise diagnosis and development of cause-directed therapies remain challenging. A major hurdle has been the lack of understanding of etiologically inciting molecular and cellular events and key pathophysiologic mechanisms that lead to autoimmunity.

A central component of autoimmunity consists of autoantigens, against which the immune system raises autoantibodies and destructive autoreactive cells. Rules that determine the repertoire of possible autoantigens and that differentiate autoantigens from the majority of nonautoantigenic self molecules are at present unknown. Among the tens of thousands of human molecules, only a small fraction (<1%) have been observed to serve as autoantigens.[1,2] At first glance, these autoantigens appear to be a *Wunderkammer*—a

Supported by grants from the National Institute of Allergy and Infectious Diseases (NIAID-NIH) (J.Y.W.) and the American Cancer Society (grant IRG-72-001-35-IRG to M.H.A.R.). M.H.A.R. is a Faculty Fellow of the Karin Grunebaum Cancer Research Foundation. W.Z. is supported in part by the Chinese Scholarship Council.

Accepted for publication January 25, 2011.

Supplemental material for this article can be found at *http://ajp.amjpathol.org* and at doi:10.1016/j.ajpath.2011.01.031.

Address reprint requests to Julia Y. Wang, Ph.D., Channing Laboratory, Department of Medicine, Brigham and Women's Hospital, 181 Longwood Ave., Boston, MA 02115; or Michael H.A. Roehrl, M.D., Ph.D., Department of Pathology and Laboratory Medicine, Boston Medical Center, 670 Albany St., Boston, MA 02118. E-mail: julia_wang@rics.bwh.harvard.edu or michael_roehrl@post.harvard.edu.

collection of curiosities without apparent unifying properties, such as physicochemical properties or functional attributes.[1] On the other hand, many autoimmune diseases share autoantigen markers and display overlapping clinical symptoms. Certain molecules, such as nuclear proteins and proteins involved in the synthesis and processing of DNA and RNA, are more prone to becoming autoantigens.[3] Autoimmune diseases also occur more frequently in females.[4] Notably, autoantibody repertoires appear similar in both human patients and mouse models.[5] These facts and other evidence suggest that autoantigenic properties of self molecules are governed by rules yet to be uncovered.

Several theories attempt to explain the origin of autoantigens. One popular theory is that autoantigens are derived from apoptotic cells, and that, during cell apoptosis, certain self molecules undergo programmed or spontaneous modifications that render them different from the native self and thus autoantigenic.[6] Another theory is that of molecular mimicry,[7] which postulates that an immune response initially aimed at a foreign antigen from a microbial infection also targets a self antigen with shared or very similar epitopes. A similar theory is that of epitope spreading.[8] A primary immune response triggered by a dominant epitope of a foreign antigen may prompt subsequent responses to other epitopes of the same molecule, and through molecular mimicry of these latter epitopes with self antigens, the immune response would spread from the exogenous antigen to self antigens. A less commonly broached theory is that autoantigens may share certain physicochemical features (not necessarily the conventional epitope *per se*). For example, long charge-rich coiled-coil segments have been found in various autoantigens.[9,10]

Here and in a companion article in this issue, we propose that affinity to dermatan sulfate (DS) is a unifying property of autoantigens. In the companion article, we demonstrate that DS physically interacts with dead cells and that the resulting DS•autoantigen complexes drive autoreactive B-1a cell responses and autoantibody production in mouse models.[11] Here, we provide further support for our hypothesis with data from human patients and report the identification of approximately 200 human autoantigens with DS affinity.

Materials and Methods

ANA/ENA Reference and Human Patient Sera

QUANTA Chek ANA (antinuclear antigen) and ENA (extractable nuclear antigen) reference panels (INOVA Diagnostics, San Diego, CA) comprise well-characterized sera from autoimmune disease patients that are known to react with a variety of specific autoantigens. Additional sera from 36 patients with known autoimmune diseases (such as SLE and Sjögren syndrome) were obtained from the Department of Pathology at Massachusetts General Hospital (Boston, MA) after Institutional Review Board approval (see Supplemental Table S1 at *http://ajp.amjpathol.org*). The presence of autoantibodies in patient sera was initially surveyed with an INNO-LIA ANA Update test kit (Innogenetics, Gent, Belgium) that detects antibodies against the following autoantigens: Sm (SmB and SmD), RNP (RNP-70k, RNP-A, RNP-C), SS-A (Ro52 and Ro60), SS-B/La, centromere (Cenp-B), Scl-70 (DNA topoisomerase I), Jo-1, ribosomal P, and histones.

Cell Culture and Protein Extraction

A549 and HFL-1 cells were cultured in F-12K medium (Invitrogen, Carlsbad, CA). HEp-2 cells were cultured in Eagle's minimum essential medium. HS-Sultan and WIL2-NS cells were cultured in RPMI-1640 medium. All media were supplemented with 10% fetal bovine serum and a penicillin-streptomycin-glutamine mixture (Invitrogen). Harvested cells were resuspended in 50 mmol/L phosphate buffer (pH 7.4) containing Roche c*O*mplete Mini protease inhibitor cocktail (Roche Diagnostics, Indianapolis, IN). Cells were homogenized on ice and then sonicated on ice for 5 minutes. The homogenate was centrifuged, and the supernatant was used as total protein extract. Protein concentrations were measured with the RC DC Protein Assay (Bio-Rad Laboratories, Hercules, CA). All samples were stored at −80°C.

DS-Affinity Chromatography

DS-Sepharose resin was prepared by coupling DS (Sigma-Aldrich, St. Louis, MO) to EAH Sepharose 4B (GE Healthcare, Piscataway, NJ). The resin (20 mL) was washed with distilled water and 0.5 mol/L NaCl and then was mixed with 100 mg of DS dissolved in 10 mL of 0.1 mol/L MES buffer (pH 5.0). *N*-ethyl-*N*-(3-dimethylaminopropyl) carbodiimide hydrochloride (Sigma-Aldrich) was added to a final concentration of 0.1 mol/L. The mixture was incubated at 25°C for 24 hours with end-over-end rotation. After the first 60 minutes, the pH was readjusted to 5.0. After the coupling, the resin was washed three times each with a low-pH buffer (0.1 mol/L acetate, 0.5 mol/L NaCl, pH 5.0) and a high-pH buffer (0.1 mol/L Tris, 0.5 mol/L NaCl, pH 8.0). The DS-Sepharose resin in 10 mmol/L phosphate buffer (pH 7.4) was packed into a C 16/20 column (GE Healthcare). Fractionation of proteins by DS affinity was performed using a BioLogic Duo-Flow system (Bio-Rad). Typically, 20 mg to 50 mg of protein extract in 40 mL of 10 mmol/L phosphate buffer (pH 7.4; buffer A) was loaded onto the DS affinity column at a rate of 1 mL/minute. The column was washed with 60 mL of buffer A to elute nonbinding proteins. DS-binding proteins were eluted with sequential 40-mL step gradients containing 0.2, 0.4, 0.6, and 1.0 mol/L NaCl. Fractions were desalted and concentrated to 0.5 mL each in 5-kDa cutoff Vivaspin 20 centrifugal filters (Sartorius Stedim Biotech, Aubagne, France). The final protein concentration of each fraction was measured. In some experiments, only two step gradients (0.5 and 1.0 mol/L NaCl) were used.

1-D and 2-D Gel Electrophoresis

For 1-D gel electrophoresis, 8 μg to 20 μg of proteins were loaded per lane and separated by SDS-PAGE with 4% to 12% NuPAGE Novex Bis-Tris gels (Invitrogen) with MES or MOPS (morpholine propane sulfonic acid) running buffer. For 2-D gel electrophoresis, 50 μg to 100 μg of proteins were cleaned with the ReadyPrep 2-D cleanup kit (Bio-Rad), redissolved in 185 μL of ReadyPrep rehydration/sample buffer (Bio-Rad) and separated on 11-cm IPG strips (pH 3 to 10; Bio-Rad) using a Protean isoelectric focusing cell (Bio-Rad). In some experiments, 7-cm IPG strips (pH 3 to 10 or pH 3 to 6) were used with 120 μL of rehydrated sample. The focused strips were equilibrated with SDS-PAGE equilibration buffers I and II (Bio-Rad). Proteins were separated along the second dimension using 8% to 16% Criterion Tris-HCl gradient gels (Bio-Rad). Fixed gels were stained with fluorescent SYPRO Ruby (Bio-Rad) for 16 hours and imaged on a Typhoon 9410 scanner (GE Healthcare). Images were analyzed with PDQuest 7.4.0 software (Bio-Rad). Gels subjected to Western blot analysis were stained with Bio-Safe Coomassie Blue G250 (Bio-Rad).

Western Blotting with ANA/ENA Reference or Patient Sera

Proteins from 1-D or 2-D gels were transferred to polyvinylidene difluoride membranes and blocked with 2% bovine serum albumin, 1% casein, and 0.5% Tween 20 in Tris-buffered saline (pH 7.4) at 25°C for 1 hour. Membranes were incubated with test serum (diluted 1:1000 or 1:2000) in blocking buffer at 25°C for 1 hour. After three washes with Tris-buffered saline containing 0.5% Tween 20, membranes were incubated with 0.2 μg/mL goat anti-human IgG conjugated with horseradish peroxidase (Santa Cruz Biotechnology, Santa Cruz, CA) at 25°C for 1 hour. Membranes were developed using enhanced chemiluminescence Western blotting substrate (Pierce; Thermo Fisher Scientific, Rockford, IL).

Protein Identification by Mass Spectrometry

Mass spectrometric (MS) sequencing was performed at the Taplin Biological Mass Spectrometry Facility (Harvard Medical School). Selected protein spots from 1-D or 2-D PAGE gels were excised and cut into 1-mm^3 pieces.[12] Gel pieces were dehydrated with acetonitrile, dried in a speed-vac concentrator, and rehydrated at 4°C for 45 minutes in 50 mmol/L NH_4HCO_3 containing 12.5 ng/μL modified sequencing-grade trypsin (Promega). Tryptic peptides were separated on a nano-scale C_{18} HPLC capillary column and analyzed after electrospray ionization in an LTQ linear ion-trap mass spectrometer (Thermo Fisher Scientific, West Palm Beach, FL).[13] Peptide sequences and protein identities were assigned by matching protein or translated nucleotide databases with the measured fragmentation pattern using SEQUEST software, version 27 (revision 12) (Therma Fisher Scientific). Peptides were required to be fully tryptic peptides with XCorr values of at least 1.5 (1^+ ion), 1.5 (2^+ ion), or 3.0 (3^+ ion). All data were manually inspected. Only proteins with ≥2 independent peptide matches were considered positively identified.

Immunoprecipitation

Patient serum samples demonstrating strong and well-separated bands on Western blots were used to determine the identities of the recognized autoantigens. Protein extracts from HEp-2 or WIL2-NS cells were fractionated by DS-affinity chromatography. Patient-specific autoantigens present in these fractions were enriched by immunoprecipitation with patient serum, separated by 1-D or 2-D electrophoresis in duplicate gels, and reactivity with patient serum was verified using Western blot analysis. Immunoprecipitation was performed with a ProFound coimmunoprecipitation kit (Pierce; Thermo Fisher Scientific), and antibodies in patient sera were covalently immobilized onto the resin. Before coupling, antibodies were typically purified from 100 μL of patient serum using a Melon gel IgG purification kit (Pierce; Thermo Fisher Scientific). In some experiments, protein A-Sepharose resin was used to noncovalently immobilize antibodies in patient sera. Protein extracts were absorbed with protein A-Sepharose to remove proteins that bind to protein A and then were incubated with autoantibody-bound protein A-Sepharose at 25°C for 1 hour. The mixture was centrifuged to precipitate autoantigen•autoantibody•protein A-Sepharose complexes. The complexes were dissociated by SDS-PAGE and examined using Western blot analysis. Reactive protein spots or bands were excised from duplicate gels and sequenced by tandem MS.

Quantification of Immunoglobulins

DS-specific IgM and IgG in patient sera were measured by enzyme-linked immunosorbent assay.[11] Nunc MaxiSorp 96-well plates were coated with 0.1 mg/mL DS or 2.5 μg/mL goat anti-human $F(ab')_2$ at 4°C overnight. Wells were blocked with 1% bovine serum albumin at 25°C for 1 hour. Patient sera were diluted 100-fold for measurement of DS-specific antibodies and 2000-fold for measurement of total Ig. IgG and IgM were detected by alkaline phosphatase-conjugated goat anti-human IgG and IgM, respectively.

Electron Microscopy

WIL2-NS cells were cultured in Dulbecco's modified Eagle's medium containing 10% fetal bovine serum (DMEM-10) with 40 μg/mL DS-biotin conjugate (in-house synthesized) for 3 days. Cells were fixed with 4% paraformaldehyde at 25°C for 30 minutes and processed as described.[11] Sections of cells were stained with goat anti-biotin conjugated to 20-nm gold particles and examined with a JEOL 1200EX transmission electron microscope (JEOLO USA, Peabody, MA).

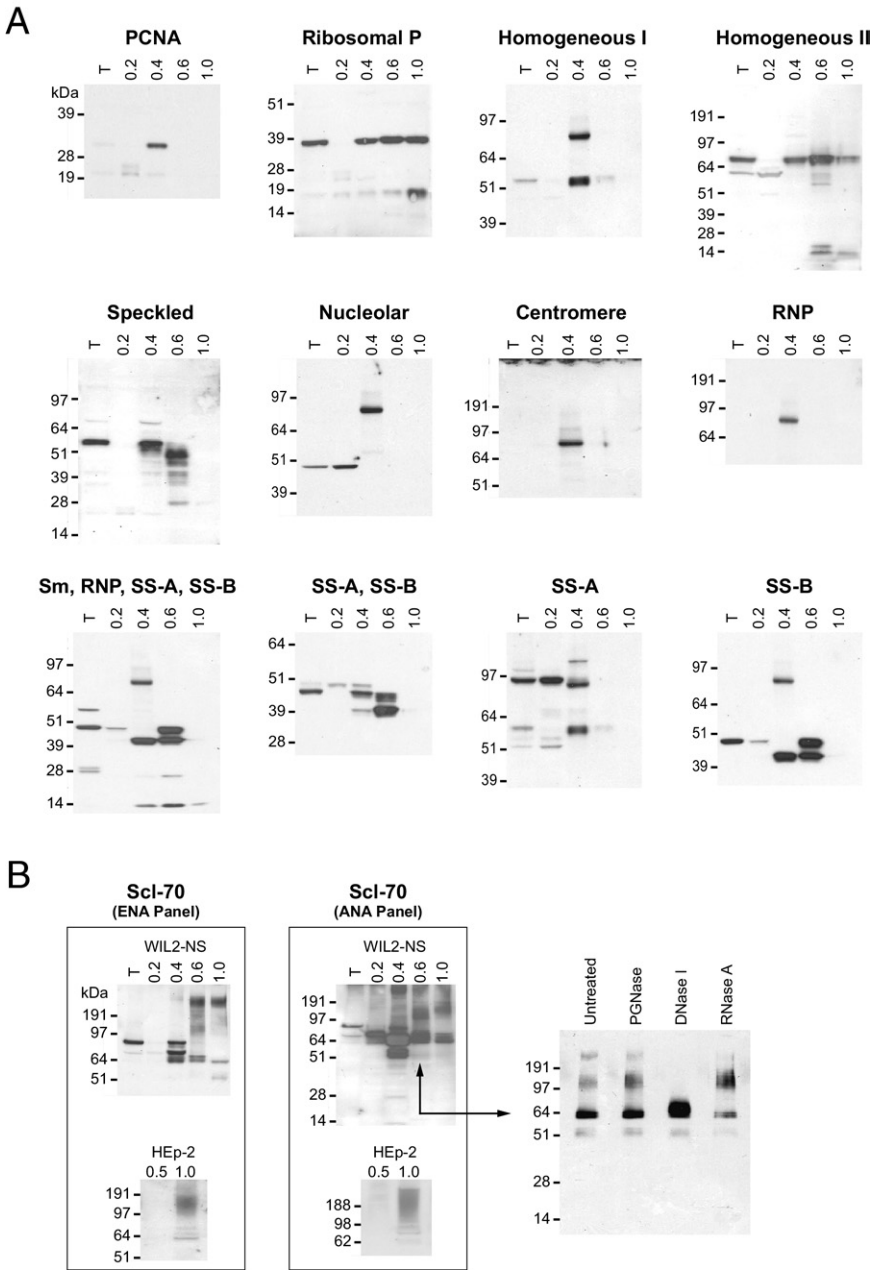

Figure 1. A: Classic ANA/ENA autoantigens are characterized by affinity to DS. Proteome extracts from WIL2-NS cells were fractionated on DS-affinity columns; 10 μg of total proteins were loaded per lane. Gels were blotted with individual ANA or ENA reference serum (each gel is labeled with the nominal reference serum specificity). **B:** DS interacts with Scl-70•DNA complexes. **Left:** ENA and ANA panels. Proteome extracts from WIL2-NS or HEp-2 cells were fractionated by DS affinity and blotted with two different Scl-70 reference sera. Note that smeared bands at high molecular weight were detected in DS-binding fractions. **Right:** For the ANA panel, WIL2-NS proteins eluted with 0.6 mol/L NaCl were treated with PNGase F, DNase I, or RNase A and analyzed by electrophoresis and using Western blot analysis with Scl-70 reference serum. Only after digestion with DNase I did the smeared bands disappear, whereas the band corresponding to Scl-70 increased in intensity, suggesting that the smear corresponds to Scl-70•DNA complexes. Lane labels: T, total unfractionated extract; numbers above lanes indicate the molar concentration of NaCl used for the respective elution step.

Results

Classic ANA/ENA Autoantigens Are Characterized by Affinity to DS

To test the hypothesis that autoantigens are characterized by affinity to DS, we first examined a panel of well-known ANA (antinuclear antigen) and ENA (extractable nuclear antigen) autoantigens. Autoantibodies against ANAs and ENAs are hallmarks of systemic autoimmune diseases, and their detection is a major screening test in clinical practice.[14] We extracted the proteomes of various human cell lines, fractionated them on a DS-affinity column with increasing concentrations of salt, and interrogated for abundance of ANA or ENA autoantigens in these fractions by blotting with ANA or ENA reference sera. Proteins eluted from the DS-affinity column with step gradients of 0.2 mol/L, 0.4 to 0.6 mol/L, or 1 mol/L NaCl were considered not/weakly DS-binding, DS-binding, or tightly DS-binding, respectively (Figure 1; see also Supplemental Figure S1 at *http://ajp.amjpathol.org*).

Because a single cell line may not express a complete repertoire of autoantigens, we examined the proteomes from five human cell lines representing different tissue types: HEp-2 (epithelial cell line used diagnostically for ANA immunofluorescence assays), A549 (epithelial), HFL-1 (mesenchymal), HS-Sultan (lymphoid), and WIL2-NS (lymphoid). Protein extracts from the different cell lines typically revealed distinct autoreactive patterns, illustrating the differential presence of various autoantigen repertoires in these cells (Figure 1; see also

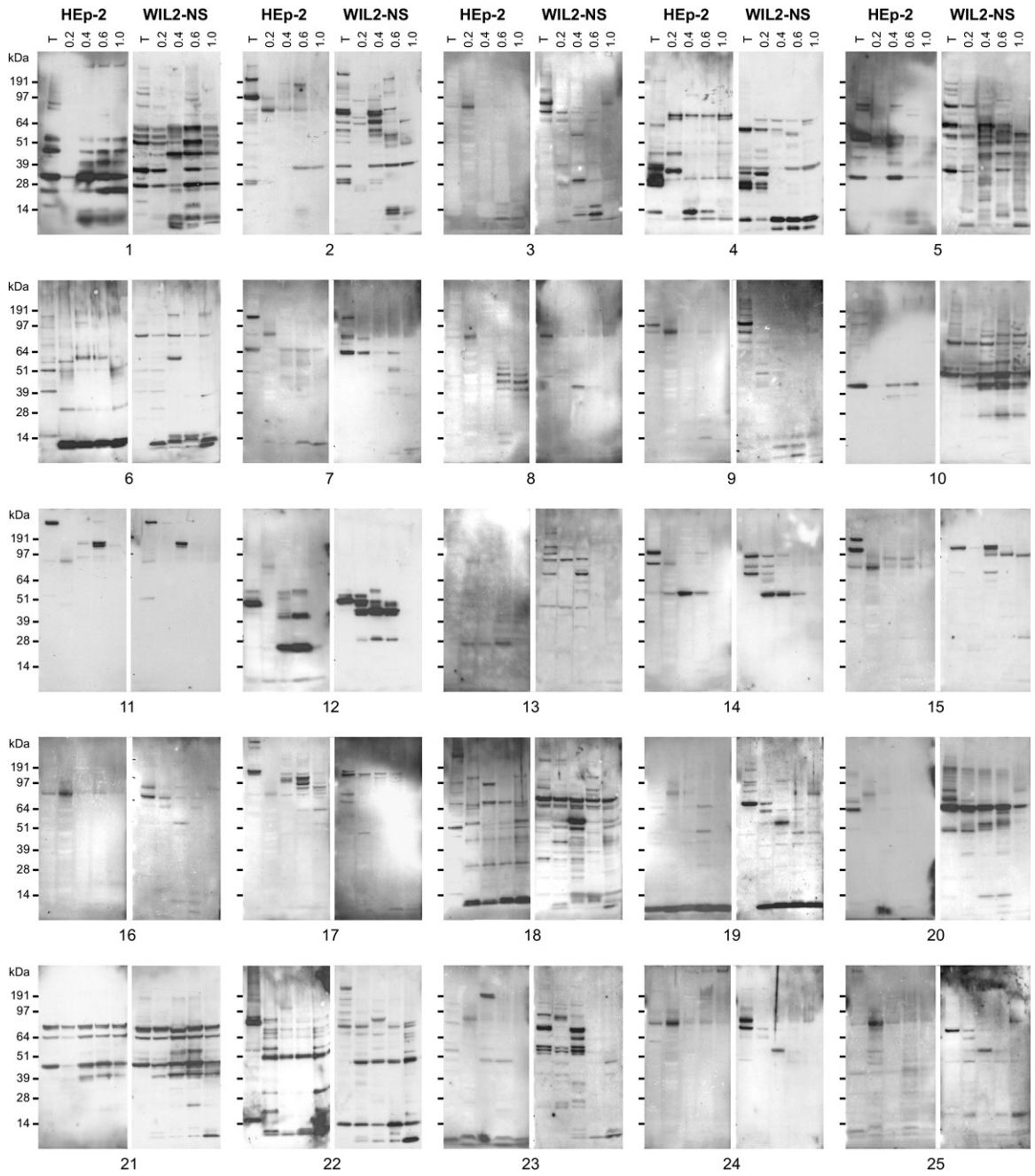

Figure 2. Autoantigen profiling in autoimmune disease shows unexpected diversity. Proteins extracted from HEp-2 or WIL2-NS cells were DS-affinity fractionated (T, total unfractionated extract; numbers above lanes indicate the molar concentration of NaCl used for the respective elution step); 8 μg of total proteins were loaded per lane. Autoantigens were detected using Western blot analysis with individual patient serum (gels for patients 1 to 25 are shown). The ~80-kDa band frequently appearing in not/weakly DS-binding (0.2 mol/L NaCl) fractions was identified as Ig γ-1 chain C (see Supplemental Figure S3D at *http://ajp.amjpathol.org*), which reacts with the secondary anti-IgG used for blotting and thus corresponds to a false positive band.

Supplemental Figure S1 at *http://ajp.amjpathol.org*). Of the five cell lines, WIL2-NS cells gave typically rise to the highest number of autoantigens and associated autoreactive bands (Figure 1A).

Remarkably, all autoantigens recognized by ANA and ENA reference antisera were present in the DS-binding or tightly DS-binding fractions (Figure 1; see also Supplemental Figure S1 at *http://ajp.amjpathol.org*). Some autoantigens were detectable only after DS-affinity fractionation; for example, PCNA (proliferating cell nuclear antigen) was detectable only in DS-binding fractions, not in unfractionated or nonbinding proteins. Similarly, autoantigens reactive with anti-RNP or anti-centromere serum were detected only in DS-binding, not in total unfractionated or nonbinding fractions. Thus, DS-affinity fractionation significantly enriched these autoantigens to detectable levels.

Total unfractionated protein extracts typically showed a single major autoantigen band corresponding to the expected specificity of each ANA or ENA reference se-

Table 1. Tandem MS Sequencing of Selected DS-binding Proteins from 1-D/2-D PAGE Gels

UniProt ID	Protein ID*	Peptide matches	MS/MS coverage (aa)	Cell line	PAGE	NaCl**
P05455	LA (La autoantigen, SS-B)	15	148/408 (36.3%)	HS-Sultan	2-D	0.4-1.0 M
P12956	KU70 (Ku autoantigen protein p70, XRCC6)	3	45/608 (7.4%)	HEp-2	1-D	0.4-0.6 M
	KU70	21	257/608 (42.3%)	HEp-2	1-D	0.4-0.6 M
P13010	KU86 (Ku autoantigen protein p86, XRCC5)	10	109/731 (14.9%)	HEp-2	1-D	0.4-0.6 M
P19338	NUCL (nucleolin)	12	122/709 (17.2%)	HEp-2	1-D	0.4-0.6 M
	NUCL	14	161/709 (22.7%)	A549	2-D	0.4-0.6 M
P06748	NPM (nucleophosmin)	16	172/294 (58.5%)	A549	2-D	0.4-0.6 M
P05388	RLA0 (60S acidic ribosomal protein P0)	10	120/317 (37.9%)	HS-Sultan	2-D	0.4-1.0 M
Q9UNX3	RL26L (60S ribosomal protein L26-like 1)	4	33/145 (22.8%)	A549	2-D	0.4-0.6 M
P46777	RL5 (60S ribosomal protein L5)	16	110/296 (37.2%)	HEp-2	1-D	0.5-1.0 M
Q96A08	H2B1A (histone H2B type 1-A)	5	42/126 (33.3%)	A549	2-D	0.4-0.6 M
P33778	H2B1B (histone H2B type 1-B)	4	25/125 (20.0%)	A549	2-D	0.4-0.6 M
Q6FGB8	Histone H4	7	54/103 (52.4%)	WIL2-NS	2-D	0.4-0.6 M
Q01105	SET (HLA-DR-associated protein II)	9	138/290 (47.6%)	A549	2-D	0.4-0.6 M
P39687	AN32A (acidic leucine-rich nuclear phosphoprotein 32 family member A)	16	130/249 (52.2%)	A549	2-D	0.4-0.6 M
Q92688	AN32B (acidic leucine-rich nuclear phosphoprotein 32 family member B)	11	57/251 (22.7%)	A549	2-D	0.4-0.6 M
P16989	DBPA (DNA-binding protein A)	4	40/372 (10.8%)	HEp-2	2-D	0.5-1.0 M
O60812	HNRCL (hnRNP core protein C-like 1)	9	73/293 (24.9%)	A549	2-D	0.4-0.6 M
	HNRCL	5	41/293 (14.0%)	WIL2-NS	2-D	0.4-0.6 M
P07910	HNRPC (heterogeneous nuclear ribonucleoproteins C1/C2)	8	95/306 (31.0%)	A549	2-D	0.4-0.6 M
Q16629	SFRS7 (splicing factor, arginine/serine-rich 7)	3	30/238 (12.6%)	WIL2-NS	2-D	0.4-0.6 M
Q15393	SF3B3 (splicing factor 3B subunit 3)	11	139/1217 (11.4%)	HEp-2	1-D	0.4-0.6 M
P12814	ACTN1 (alpha-actinin-1)	28	334/892 (37.4%)	HEp-2	1-D	0.4-0.6 M
O43707	ACTN4 (alpha-actinin-4)	22	270/911 (29.6%)	HEp-2	1-D	0.4-0.6 M
Q13813	SPTA2 (spectrin alpha chain, brain)	17	233/2472 (9.4%)	HEp-2	1-D	0.4-0.6 M
P27797	Calreticulin	19	209/417 (50.1%)	HEp-2	2-D	0.5-1.0 M
	Calreticulin	15	180/417 (43.2%)	HEp-2	2-D	0.2-0.4 M
Q07021	C1QBP (complement component 1 Q subcomponent-binding protein, mitochondrial)	3	58/282 (20.6%)	HEp-2	2-D	0.5-1.0 M
	C1QBP	12	171/282 (60.6%)	A549	2-D	0.4-0.6 M
	C1QBP	8	115/282 (40.8%)	HS-Sultan	2-D	0.4-1.0 M
Q13310	PABP4 (poly(A)-binding protein 4)	16	136/644 (21.1%)	HEp-2	1-D	0.5-1.0 M
Q9H361	PABP3 (poly(A)-binding protein 3)	9	77/631 (12.2%)	HEp-2	1-D	0.5-1.0 M
P11021	GRP78 (heat shock 70 kDa protein 5)	51	401/654 (61.3%)	A549	2-D	0.5-1.0 M
	GRP78	16	214/654 (32.7%)	HEp-2	1-D	0.4-0.6 M
	GRP78	34	336/654 (51.4%)	HEp-2	2-D	0.2-0.4 M
P11142	HSP7C (heat shock cognate 71 kDa protein)	15	193/646 (29.9%)	HEp-2	2-D	0.5-1.0 M
	HSP7C	6	91/646 (14.1%)	HEp-2	2-D	0.5-1.0 M
	HSP7C	20	252/646 (39.0%)	HS-Sultan	2-D	0.4-1.0 M
P38646	GRP75 (heat shock 70 kDa protein 9)	25	338/679 (49.8%)	HEp-2	2-D	0.5-1.0 M
	GRP75	19	250/679 (36.8%)	HS-Sultan	2-D	0.4-1.0 M
P22314	UBA1 (ubiquitin-like modifier-activating enzyme 1)	15	216/1058 (20.4%)	HEp-2	1-D	0.4-0.6 M
P06733	ENOA (alpha-enolase)	12	128/433 (29.6%)	HEp-2	1-D	0.4-0.6 M
P28072	PSB6 (proteasome subunit beta type-6)	13	137/239 (57.3%)	A549	2-D	0.2-0.4 M
P21333	FLNA (filamin-A)	11	159/2646 (6.0%)	HEp-2	1-D	0.5-1.0 M
	FLNA	21	245/2646 (9.3%)	HEp-2	1-D	0.4-0.6 M
	FLNA	10	135/2646 (5.1%)	HEp-2	1-D	0.4-0.6 M
O75369	FLNB (filamin-B, thyroid autoantigen)	17	217/2602 (8.3%)	HEp-2	1-D	0.4-0.6 M
Q6P2Q9	PRP8 (pre-mRNA-processing-splicing factor 8)	12	119/2335 (5.1%)	HEp-2	1-D	0.4-0.6 M
P62306	RUXF (snRNP-F)	7	27/86 (31.4%)	A549	2-D	0.4-0.6 M
Q53GF5	Proteasome subunit alpha type	13	128/234 (54.7%)	A549	2-D	0.2-0.4 M
P25789	PSA4 (proteasome subunit alpha type-4)	20	197/261 (75.5%)	A549	2-D	0.2-0.4 M
Q16531	DDB1 (damage-specific DNA-binding protein 1)	28	295/1140 (25.9%)	HEp-2	1-D	0.4-0.6 M
Q00577	PURA (purine-rich single-stranded DNA-binding protein alpha)	7	110/322 (34.2%)	A549	2-D	0.4-0.6 M
Q04837	SSBP (single-stranded DNA-binding protein, mitochondrial)	10	89/148 (60.1%)	A549	2-D	0.4-0.6 M
	SSBP	10	93/148 (62.8%)	WIL2-NS	2-D	0.4-0.6 M
	SSBP	5	52/148 (35.1%)	WIL2-NS	2-D	0.4-0.6 M
Q00610	CLH1 (clathrin heavy chain 1)	51	565/1674 (33.8%)	HEp-2	1-D	0.4-0.6 M
P80723	BASP1 (brain acid soluble protein 1)	3	49/226 (21.7%)	HEp-2	2-D	0.2-0.4 M
P02765	FETUA (fetuin A, alpha-2-HS-glycoprotein)	2	13/367 (3.5%)	HEp-2	2-D	0.2-0.4 M
P07148	FABPL (fatty acid-binding protein, liver)	5	67/127 (52.8%)	WIL2-NS	2-D	0.4-0.6 M
	FABPL	3	35/127 (27.6%)	WIL2-NS	2-D	0.4-0.6 M
Q6ZRT8	Ubiquitin C	5	43/186 (23.1%)	WIL2-NS	2-D	0.4-0.6 M

A complete version of the table, with literature references characterizing the proteins as functional human autoantigens, can be found in the Supplemental Appendix (available at *http://ajp.amjpathol.org*).

*Repeated listing of the same protein indicates that tandem MS sequencing of more than one gel band/spot yielded the same protein identity.

**NaCl concentrations used to wash and elute from DS-affinity resin (eg, 0.4-1.0 M indicates that proteins were eluted with 1.0 M NaCl after washing with 0.4 M NaCl).

rum (Figure 1). After DS-affinity fractionation, however, numerous additional autoantigen bands became detectable that had not previously been known to be recognized by these reference sera. For example, instead of one major band (in unfractionated extract), ANA reference serum (with speckled immunofluorescence reactivity pattern) recognized numerous bands in the 0.4 mol/L and 0.6 mol/L NaCl fractions (Figure 1). Similarly, addi-

Table 2. Tandem MS Sequencing of DS-associating Proteins and Their Known Autoantigenic Propensities

Peptide matches*				
1.0-M NaCl fraction	0.6-M NaCl fraction	0.4-M NaCl fraction	UniProt ID	Protein ID
				Chromatin-related proteins
6,7	5,4,4,6	4,5,5	Q6FGB8	Histone H4
5,2	5		P33778	Histone H2B type 1-B
3	2,4		Q96A08	Histone H2B type 1-A testis-specific histone H2B
2	3,4		Q96QV6	Histone H2A type 1-A
4	2,3	2	Q16695	Histone H3.4
2	6,3,2	3	P16401	Histone H1.5 histone H1A
2	2	3	Q02539	Histone H1.1
	2	2,2	P16403	Histone H1.2 histone H1D
		6,3,2	P49321	Nuclear autoantigenic sperm protein histone binding protein
		2	Q16576	Histone-binding protein rbbp7 retinoblastoma-binding protein 7
2	3		P16989	DNA-binding protein A cold shock domain-containing protein A, single-strand DNA-binding protein NF-GMB
2		3,4,3	P53999	Activated RNA polymerase II transcriptional coactivator p15
3			Q6PKI6	YBX1 protein transcription factor
2			Q96E14	Hypothetical protein RecQ-mediated genome instability protein 2, BLM-associated protein of 18 kDa
2	5,5,4		Q01105	SET phosphatase 2a inhibitor, HLA-DR-associated protein II
	9,10,10		P39687	Acidic leucine-rich nuclear phosphoprotein 32 family member A potent heat-stable protein phosphatase 2A inhibitor I1PP2A
	5,4,5		Q92688	Acidic leucine-rich nuclear phosphoprotein 32 family member B
	3,2,2		Q9BTT0	Acidic leucine-rich nuclear phosphoprotein 32 family member E
	4,2	2,3,3	P55209	Nucleosome assembly protein 1-like 1
	7	2	Q99733	Nucleosome assembly protein 1-like 4
	5,2	5,3,4	P13010	ATP-dependent DNA helicase 2 subunit 2 Ku autoantigen protein p86
	8,2	4,12,7	P12956	ATP-dependent DNA helicase 2 subunit 1 Ku autoantigen protein p70
	4,3	3,3,4	P06454	Prothymosin alpha
	2		Q08945	FACT complex subunit SSRP1 facilitates chromatin transcription complex subunit SSRP1
	2		Q9Y5B9	FACT complex subunit SPT16 facilitates chromatin transcription complex subunit SPT16
		9,6,6	Q9UGV6	High mobility group protein 1-like 10
		5,2,5,3	P51858	Hepatoma-derived growth factor high-mobility group protein 1-like 2
		2	Q75MM1	Similar to non-histone chromosomal protein HMG-1
		3,9,3	P49736	DNA replication licensing factor MCM2 minichromosome maintenance protein 2 homolog
		3,7	Q14566	DNA replication licensing factor MCM6
		3,4	P33991	DNA replication licensing factor MCM4
		2,3	P25205	DNA replication licensing factor MCM3
		3	P33992	DNA replication licensing factor MCM5
		3,2,2	Q13185	Chromobox protein homolog 3 heterochromatin protein 1 homolog gamma
		2	P83916	Chromobox protein homolog 1 heterochromatin protein 1 homolog beta
		3	P78527	DNA-dependent protein kinase catalytic subunit
		3	P20290	Transcription factor BTF3 RNA polymerase B transcription factor 3
		2	P35659	Protein DEK
		6,5,2	P12004	Proliferating cell nuclear antigen PCNA
		2	P11387	DNA topoisomerase 1 Scl-70
				Nucleolar phosphoproteins
4	23,17,17,3	3,6,3	P19338	Nucleolin
2	6,4,2	2,6,4	P06748	Nucleophosmin
	7,3		Q14978	Nucleolar phosphoprotein p130 nucleolar and coiled-body phosphoprotein 1
	2		Q9BQG0	Myb-binding protein 1A
				Nuclear pore complex-related proteins
		7,3	O00410	Importin subunit beta-3 karyopherin subunit beta-3
		6	Q14974	Importin subunit beta-1 karyopherin subunit beta-1
		2	O00505	Importin subunit alpha-3 karyopherin subunit alpha-3
		2	O43592	Exportin-T tRNA exportin
				Ribonucleoproteins RNPs or ribosomal proteins
2	3		P05388	60S acidic ribosomal protein P0
2,3		3,4,2,2	P05387	60S acidic ribosomal protein P2
7	2,3		P18124	60S ribosomal protein L7
6	7,7,2		P46777	60S ribosomal protein L5
4	2,2		P62424	60S ribosomal protein L7a
4	2,3		Q02878	60S ribosomal protein L6
2	2,2		Q9NQS8	Ribosomal protein S3
2	2		P62753	40S ribosomal protein S6
2	2		P15880	40S ribosomal protein S2 S4
5	4		P46781	40S ribosomal protein S9
2	2		P62244	40S ribosomal protein S15a
2	3		Q6NXR8	Ribosomal protein S3A
2	2		P82663	Ribosomal protein S25
2	3		Q6IPX9	Ribosomal protein S3
2			Q5T6E0	Ribosomal protein L15
2			Q9UNX3	60S ribosomal protein L26-like 1
3			P39023	60S ribosomal protein L3
2			Q07020	60S ribosomal protein L18
2			Q59FI9	Ribosomal protein L12 variant
	2,2	2	P35268	60S ribosomal protein L22
	2		U02032	Ribosomal protein L23a
	2		Q6IRZ0	RPL31 protein
	2		Q567Q7	Ribosomal protein L8
		3,2	M77233	Ribosomal protein S7
2,3	4,6,4	2,6,4	P05455	Lupus La protein SS-B
6,2,2			Q9H361	Polyadenylate-binding protein 3
2			Q13310	Polyadenylate-binding protein 4
2	8,2,4		P09661	U2 small nuclear ribonucleoprotein A′

(*table continues*)

Table 2. *Continued*

Peptide matches*				
1.0-M NaCl fraction	0.6-M NaCl fraction	0.4-M NaCl fraction	UniProt ID	Protein ID
				Ribonucleoproteins RNPs or ribosomal proteins
2	2	3	P62316	Small nuclear ribonucleoprotein Sm D2
4			O43818	U3 small nucleolar RNA-interacting protein 2
2			Q5VYJ4	Small nuclear ribonucleoprotein polypeptide E-like protein 1
	3		P08579	U2 small nuclear ribonucleoprotein B″
		3,2	P08621	U1 small nuclear ribonucleoprotein 70 kDa
		2	Q15029	U5 snRNP-specific protein, 116 kDa
2	2,3		O60812	hnRNP core protein C-like 1
	2,3		P07910	hnRNPs C1/C2
	2	2,2	P31943	hnRNP H
		3,3,2	O43390	hnRNP R
		6,6	O60506	hnRNP Q
		2,5	Q00839>	hnRNP U
		7	P61978	hnRNP K
		3	P09651	hnRNP core protein A1
		2	Q14103	hnRNP D0
		2	P22626	hnRNPs A2/B1
	2		Q9NR30	Nucleolar RNA helicase 2
		9,4	Q9BRB1	Hypothetical protein DEAD box helicase family
		5,5	O00148	ATP-dependent RNA helicase DDX39
		3,2	Q13838	Spliceosome RNA helicase BAT1
		2	Q08211	ATP-dependent RNA helicase A
	3,2		Q16629	Splicing factor, arginine/serine-rich 7
	4		Q08170	Splicing factor, arginine/serine-rich 4
	3	4,3	Q07955	Splicing factor, arginine/serine-rich 1
	2		Q53FN0	Splicing factor, arginine/serine-rich 2 variant
	2		Q13247	Splicing factor, arginine/serine-rich 6
	2		Q13243	Splicing factor, arginine/serine-rich 5
	2		Q96TA3	SRP46 splicing factor
		4,3,2	Q15393	Splicing factor 3B subunit 3
		2,2	Q15459	Splicing factor 3 subunit 1
2			P49458	Signal recognition particle 9 kDa protein
	2		Q9UHB9	Signal recognition particle 68 kDa protein
	3		Q99613	Eukaryotic translation initiation factor 3 subunit 8
	2		O60841	Eukaryotic translation initiation factor 5B
		2,2	P56537	Eukaryotic translation initiation factor 6
		2	P05198	Eukaryotic translation initiation factor 2 subunit 1
		2	Q04637	Eukaryotic translation initiation factor 4 gamma 1
		2	Q9GZV4	Eukaryotic translation initiation factor 5A-2
		2	P60228	Eukaryotic translation initiation factor 3 subunit 6
		2	Q9Y262	Eukaryotic translation initiation factor 3 subunit L
				Cytoskeletal proteins
6	10,3	12,9,4	P08670	Vimentin
2	4	2,3,2	Q5T8M8	Actin, alpha 1, skeletal muscle
3	2,2	4,2	Q6PJ43	Actin, gamma 1
	2	2,2	Q9BYX7	Kappa actin
		4,7,3	P12814	Alpha-actinin-1
		2,6,5	O43707	Alpha-actinin-4
		4,2	P61758	Prefoldin subunit 3 VHL-binding protein 1
		3	Q9Y490	Talin-1
		15	P13796	Plastin-2
		3,3,3	Q8NAG3	Tropomyosin, cytoskeletal type
		3,3,3	P06753	Tropomyosin alpha-3 chain
		2,4,2	P09493	Tropomyosin alpha-1 chain
		6,4	P67936	Tropomyosin alpha-4 chain
		2	P07951	Tropomyosin beta chain
		2,3	P35579	Myosin-9
		3	Q13813	Spectrin alpha chain, brain
		2	Q01082	Spectrin beta chain, brain 1
		3	P07737	Profilin-1
		2	P23528	Cofilin-1
2	6	4,6,3	Q13748	Tubulin alpha-2 chain
2	3	4,4,4	Q6LC01	Beta-tubulin
	2	2	Q9H4B7	Tubulin beta-1 chain
	2	2,2	Q9BQE3	Tubulin alpha-6 chain
		2	Q14166	Tubulin-tyrosine ligase-like protein 12
2		8	P20700	Lamin-B1
		16,11,17	P10809	60 kDa heat shock protein, mitochondrial precursor HSP60
		7	Q9Y266	Nuclear migration protein nudC nuclear distribution protein C homolog
		2	Q15691	Microtubule-associated protein RP/EB family member 1 APC-binding protein EB1
		2	Q9Y265	49 kDa TATA box-binding protein-interacting protein
				Heat shock or stress proteins
8,5	9,2	25,35,25,7	P07900	Heat shock protein HSP 90-alpha
5,7	4,9,3	15,10	P11021	Heat shock 70 kDa protein 5
5,6	2,5	4,4	P11142	Heat shock 70 kDa protein 8
2			P54652	Heat shock 70 kDa protein 2
	2	18,17,17,2	P14625	Heat shock protein 90 kDa beta member 1
	4,2	13,13,10,6	P08238	Heat shock protein HSP 90-beta
	2	2	P38646	Stress-70 protein, mitochondrial
		14,7,2	Q92598	Heat shock protein 105 kDa
		7,5,2	Q16543	HSP90 co-chaperone Cdc37
		6,6,3	P50502	Hsc70-interacting protein
		4,2	P34932	Heat shock 70 kDa protein 4

(*table continues*)

Table 2. *Continued*

Peptide matches*				
1.0-M NaCl fraction	0.6-M NaCl fraction	0.4-M NaCl fraction	UniProt ID	Protein ID
				Protein processing-related proteins synthesis, folding, degradation
	3	2,2	P29692	Elongation factor 1-delta
	3	2	P26641	Elongation factor 1-gamma
	2		P13639	Elongation factor 2
		2	P24534	Elongation factor 1-beta
		4,4	Q13765	Nascent polypeptide-associated complex subunit alpha
		12,7,3	P78371	T-complex protein 1 subunit beta
		11,11,6	P50990	T-complex protein 1 subunit theta
		5,6,2	P17987	T-complex protein 1 subunit alpha
		4,5,2	P40227	T-complex protein 1 subunit zeta
		4,5,2	Q99832	T-complex protein 1 subunit eta
		5,9	P49368	T-complex protein 1 subunit gamma
		3,7	P48643>	T-complex protein 1 subunit epsilon
		2	P50991	T-complex protein 1 subunit delta
		12,8,8,3	P07237	Protein disulfide-isomerase
		9,11,9	P13667	Protein disulfide-isomerase A4
		6,7,5	Q15084	Protein disulfide-isomerase A6
		2	O43396	Thioredoxin-like protein 1
		2,5	P28070	Proteasome subunit beta type-4
		2,4	P28066	Proteasome subunit alpha type-5
		3,2	Q8TAA3	Proteasome subunit alpha type-7-like
		3	P25786	Proteasome subunit alpha type-1
		2	O14818	Proteasome subunit alpha type-7
		2	P61289	Proteasome activator complex subunit 3
		2	Q53FT5	Proteasome 26S non-ATPase subunit 11 variant
		2	P28072	Proteasome subunit beta type-6
		2,2	Q9UBE0	SUMO-activating enzyme subunit 1
		2,2	Q9UBT2	SUMO-activating enzyme subunit 2
		10	P22314	Ubiquitin-like modifier-activating enzyme 1
		2	P45974	Ubiquitin carboxyl-terminal hydrolase 5
		2,2	Q86VP6	Cullin-associated NEDD8-dissociated protein 1
				Enzymes
2	2	4	P04406	Glyceraldehyde-3-phosphate dehydrogenase
	3,3		Q5U5J2	Casein kinase 2, alpha 1
	2,2		P46060	Ran GTPase-activating protein 1
	3		O15355	Protein phosphatase 1G
	4		P06733	Alpha-enolase
	2		P60174	Triosephosphate isomerase
	2		P40925	Malate dehydrogenase, cytoplasmic
	2	2	P00338	L-lactate dehydrogenase A chain
		3	P07195	L-lactate dehydrogenase B chain
		4,2	P30153	Serine/threonine-protein phosphatase 2A 65 kDa regulatory subunit A alpha isoform
		13,15,15,3	P55072	Transitional endoplasmic reticulum ATPase
		7,3	O95671	N-acetylserotonin O-methyltransferase-like protein
		3,3,5	Q96HY3	CALM1 protein
		2	Q9BRL5	CALM3 protein
		3,2,2	Q9Y2B0	Protein canopy homolog 2
		2,2	P14314	Glucosidase 2 subunit beta
		2	P29966	Myristoylated alanine-rich C-kinase substrate
		10	P06576	ATP synthase subunit beta, mitochondrial
		6	P49327	Fatty acid synthase
		5	Q99873	Protein arginine N-methyltransferase 1
		3	Q9Y4L1	Hypoxia-upregulated protein 1
		3	Q9UKK9	ADP-sugar pyrophosphatase
		2	P12268	Inosine-5′-monophosphate dehydrogenase 2
		2	P31939	Bifunctional purine biosynthesis protein PURH
		2	Q01581	Hydroxymethylglutaryl-coa synthase, cytoplasmic
		2	Q9NQW7	Xaa-Pro aminopeptidase 1
		2	Q15185	Prostaglandin E synthase 3
				Miscellaneous
3	3	3,2	Q07021	Complement component 1 Q subcomponent-binding protein, mitochondrial
		10,9,5,3	P27797	Calreticulin
		16	P08133	Annexin A6
		5,5	P42704	Leucine-rich PPR motif-containing protein, mitochondrial
		6,2	Q12906	Interleukin enhancer-binding factor 3
		4	Q12905	Interleukin enhancer-binding factor 2
		3	O00299	Chloride intracellular channel protein 1
		11,9,9,2	Q4VJB6	14-3-3 protein epsilon isoform transcript variant 1
		11,9,7	P31946	14-3-3 protein beta/alpha
		7,3,3	P61981	14-3-3 protein gamma
		4,5,3	Q04917	14-3-3 protein eta
		2,2,2	Q6LD62	14-3-3 protein
		2,2,2	Q2F831	14-3-3 protein zeta
		3,2,2	Q53S41	14-3-3 protein theta
		2	P62258	14-3-3 protein epsilon
		3	Q14444	Caprin-1
		2	Q9NR28	Diablo homolog, mitochondrial
		2	Q9BZZ5>	Apoptosis inhibitor 5
		2	Q8IXQ4	Lipopolysaccharide-specific response protein 7

A complete version of the table, with literature references characterizing the proteins as a functional human autoantigens, can be found in the Supplemental Appendix (available at *http://ajp.amjpathol.org*).

*Number of distinctly matched peptides that identify each protein. Four independent experiments (DS-affinity fractionation with tandem MS sequencing) were performed. Only results with positive protein identification (≥2 matched peptides) are listed. Hence, up to 4 numbers are shown in each column entry.

tional autoantigens were revealed by reference antisera with nominal specificities for SS-B, SS-A/SS-B, Scl-70, and ribosomal P. In some cases, autoreactive bands were also detected in the 0.2 mol/L NaCl fraction (Figure 1), possibly because of weak affinity of these autoantigens to DS or, particularly when the same bands were also present in higher-salt fractions, because of capacity overloading of the DS-affinity column.

The increased sensitivity of autoantigen detection by DS-affinity enrichment enabled further differentiation of traditional ANA/ENA immunofluorescence reactivity patterns. For example, two reference sera, each with homogeneous reactivity pattern in the HEp-2-based immunofluorescence assay and thus phenotypically indistinguishable, yielded very different underlying autoantigen profiles (Figure 1). Similarly, two reference sera with nominal anti-Scl-70 specificity yielded complicated and distinct profiles (Figure 1B).

These experiments also pointed to a potential mechanism for autoantigenicity of DNA. In addition to discrete protein bands, the two anti-Scl-70 sera reacted with smeared bands at high molecular weight in the DS-binding fractions from both HEp-2 and WIL2-NS proteome extracts (Figure 1B). Scl-70 (topoisomerase I) is an enzyme that unwinds supercoiled DNA by nicking and ligating DNA strands. Only DNase digestion, but not treatment with PNGase F or RNase A, caused the disappearance of the high molecular weight smears, identifying them as Scl-70•DNA complexes (Figure 1B). Thus, DS interacts not only with Scl-70 alone, but also with Scl-70•DNA complexes. In fact, it seems attractive to speculate that DS•Scl-70•DNA ternary complexes may be responsible for the production of autoantibodies to both Scl-70 and DNA.

Autoantigen Profiling in Autoimmune Disease Shows Unexpected Diversity

We next asked whether autoantigen affinity to DS could be used as a principle for comprehensive profiling of autoantigens in human autoimmune diseases. We collected sera from 36 patients with autoimmune diseases, including SLE and Sjögren syndrome, among others (see Supplemental Table S1 at *http://ajp.amjpathol.org*). Proteins extracted from HEp-2 or WIL2-NS cells were fractionated by DS affinity, separated by SDS-PAGE, and blotted with individual patient serum (Figure 2 and data not shown).

The unexpectedly complex autoreactive patterns observed were largely unique for each patient (Figure 2). Compared with a limited spectrum of clinical diagnoses (see Supplemental Table S1 at *http://ajp.amjpathol.org*) and a commercial strip assay (see Supplemental Figure S2 at *http://ajp.amjpathol.org*) that demonstrated only a small set of autoantigens, our method uncovered a much larger repertoire of autoantigens. The patient-specific autoreactive profiles illustrate an autoantigenic diversity in autoimmune diseases that is much greater than previously thought or currently assayed for. Even within patient groups with similar clinical presentation (eg, patients diagnosed with SLE), autoantigen profiles were strikingly different (Figure 2; see also Supplemental Table S1 at *http://ajp.amjpathol.org*).

When unfractionated protein extracts from either HEp-2 or WIL2-NS were used, typically only very few bands reacted with patient sera. After DS-affinity fractionation, however, numerous additional autoreactive bands emerged, particularly in DS-binding fractions. Many patients presented complex patterns with many distinct autoantigens present across the DS-binding fractions (eg, patients 1, 5, 10, 18, and 22) (Figure 2). Without DS-affinity enrichment, this large number of additional autoantigens would not have been detectable.

WIL2-NS proteome extracts generally revealed more reactive bands, and so contained more autoantigens than HEp-2 extracts. For example, serum from patient 10 reacted with two bands using fractionated HEp-2 proteins, but many more bands when proteins from WIL2-NS cells were used (Figure 2). This observation is particularly noteworthy and relevant because virtually all current clinical patient testing, including immunofluorescence pattern description, is based on HEp-2 cells, and thus likely misses a significant number of autoantibodies.

To verify that the newly detected autoreactive bands indeed resulted from specific recognition of autoantigens by patient sera, we characterized selected prominent bands in detail. Sera from patients 11, 12, and 14 (all with speckled HEp-2 ANA immunofluorescence pattern) reacted strongly with distinct bands in DS-binding fractions (Figure 2; see also Supplemental Figure S3, A–C at *http://ajp.amjpathol.org*). Proteins from HEp-2 cells were fractionated by DS affinity, and the specific reactive proteins were further enriched by serum immunoprecipitation and identified by MS sequencing (see Supplemental Figure S3 at *http://ajp.amjpathol.org*). Serum from patient 11 reacted with two bands in DS-binding fractions (0.6 mol/L NaCl), which corresponded to SPTA2 (spectrin α-II) and PRP8 (U5 snRNP) (upper band) and α-actinin-1 and α-actinin-4 (lower band) (see Supplemental Figure S3A at *http://ajp.amjpathol.org*). Serum from patient 12 reacted with LA (La/SS-B protein) (0.4 to 0.6 mol/L NaCl; see Supplemental Figure S3B at *http://ajp.amjpathol.org*. Serum from patient 14 reacted with BASP1 (brain acid soluble protein 1) and FETUA (fetuin A) (0.4 to 0.6 mol/L NaCl; see also Supplemental Figure S3C at *http://ajp.amjpathol.org*). Of note, all of these proteins serve as well-known autoantigens (Table 1; see also Supplemental Appendix and references therein at *http://ajp.amjpathol.org*), supporting the usefulness of DS affinity as a tool for enhanced profiling of autoantigens.

We next examined sera from three SLE patients (1, 2, and 7) to survey possible disease markers. Serum from patient 1 recognized several autoantigens that were detectable only after DS-affinity enrichment (Figure 2). To further characterize these specific autoantigens, DS-binding proteins from WIL2-NS cells were enriched by serum immunoprecipitation. Ten autoantigens were identified by MS sequencing: histones H1.1 and H1.5, Sm D2, U2 snRNP B″, snRNP F, La/SS-B, prothymosin α, YBX1, and 60S ribosomal proteins L6 and L5.

For patient 2, MS sequencing revealed serum specificities for 15 autoantigens, including 5 histones (H2A type 1-A, H4, H2B type 1-B, H1.5, and H2B type 1-C/E/F/G/I), 7 small nucleoprotein autoantigens (Sm D1, Sm D2, Sm D3, U1 snRNP A, U2 snRNP A′, snRNP B/B′, and U2 snRNP B″), 2 S100 calcium-binding proteins (A8 and A9), and Ig mu heavy chain binding protein. The results are consistent with a strip screening test that identified reactivity of this patient's serum with SmB, SmD, RNP-70k, RNP-A, RNP-C, and histones (see Supplemental Figure S2 at *http://ajp.amjpathol.org*).

For patient 7, five autoantigens were identified by MS sequencing: vitamin K-dependent protein S, complement C4-A, C1QBP, H2A type 1-A, and H2B type 1-B. Protein S is a known autoantigen with close links to phospholipid autoantibodies and SLE.[15]

Comparison of these SLE patients shows that patients 1 and 2 share three autoantigens (H1.5, Sm D2, and U2 snRNP B″) and patients 2 and 7 share two autoantigens (H2A type 1-A and H2B type 1-B). Of note, although patients 1, 2, 7, 11, 12, and 14 all displayed a morphologically indistinguishable speckled ANA immunofluorescence pattern on HEp-2 cells, the underlying causative autoantigen repertoires are quite divergent, another finding that highlights significant interindividual autoantigenic diversity in autoimmune diseases.

Autoantigen Repertoire (the Autoantigen-ome)

Using patient or ANA/ENA reference sera, we demonstrated that autoantigens are preferentially DS-binding. We next asked whether affinity to DS is a unifying physicochemical property of autoantigens (the autoantigen-ome).

To this end, we sought to identify potential autoantigens without use of sera from autoimmune disease patients. First, we characterized a limited number of DS-binding proteins and asked whether they had known autoantigenic propensity. Proteins extracted from several cell lines were fractionated by DS affinity and separated by 1-D or 2-D gel electrophoresis. Discrete bands or spots were then selected based on favorable separation and intensity characteristics and individually sequenced by tandem MS (Table 1; see also Supplemental Appendix and references therein at *http://ajp.amjpathol.org*).

Using A549 cells as an example, 13 spots from gels with DS-binding proteins were selected after 2-D separation, from which 18 different proteins were identified (Table 1; see also Supplemental Appendix and references therein and Supplemental Figure S4A at *http://ajp.amjpathol.org*). Using 1-D gel electrophoresis, 12 bands were sequenced, from which 23 different proteins were identified (Table 1; see also Supplemental Appendix and references therein and Supplemental Figure S4B at *http://ajp.amjpathol.org*). Some of these proteins were repeatedly identified from extracts of different cell lines or from different protein bands or spots of the same cell line (Table 1; see also Supplemental Appendix and references therein at *http://ajp.amjpathol.org*).

All 46 proteins identified in this manner are either previously known autoantigens or have been functionally associated with autoimmune diseases (Table 1; see also the Supplemental Appendix and references therein at *http://ajp.amjpathol.org*). Well-known autoantigens identified include La (a signature autoantigen in Sjögren syndrome) and the lupus autoantigens Ku70 and Ku86. Other well-established autoantigens include histones, hnRNPs, GRP78, HSP7C, filamin-A, filamin-B, nucleolin, PRP8, RLA0, and α-actinin-1 and -4. Although some of the remaining proteins have not previously been definitively characterized as autoantigens, most are, nevertheless, at least closely related to autoimmunity. For example, calreticulin shares sequence homology with GRP78 and cross-reacts with anti-Ro/SS-A.[16] Poly(A)-binding proteins 3 and 4 share sequence homology with La/SS-B.[17,18]

Next, we used a shotgun approach and sequenced pools of proteins fractionated by DS-affinity columns to characterize a much broader repertoire of potential cellular DS-binding autoantigens. Proteins from WIL2-NS cells were used because these cells express many autoantigens (Figure 1). To demonstrate the relative enrichment of autoantigens by DS affinity, we individually sequenced total, unfractionated, and fractionated pools by tandem MS.

Unfractionated proteins yielded the identities of 120 distinct proteins (see Supplemental Table S2 at *http://ajp.amjpathol.org*) from 337 2-D gel spots (see Supplemental Figure S5 and Supplemental Table S3 at *http://ajp.amjpathol.org*). Of these 120 proteins, 64 were present in DS-binding fractions (eluting with 0.4, 0.6, or 1 mol/L NaCl), 29 were in the 0.2 mol/L NaCl fraction, and 27 were not identified after fractionation. Of the total, 72 (60%) have previously been characterized as functional autoantigens.

The 0.2 mol/L NaCl fraction (ie, DS nonbinding to weakly binding) yielded 175 protein identities (see Supplemental Table S3 at *http://ajp.amjpathol.org* and references therein). Among these, 112 proteins were present exclusively in the 0.2 mol/L NaCl fraction, corresponding to nonbinding or weakly DS-binding proteins, whereas 63 were also present in fractions eluted with higher concentrations of NaCl (0.4 mol/L to 1.0 mol/L), possibly indicating biochemical heterogeneity due to post-translational modifications or excess of column loading capacity. The most abundant species among these nonbinding proteins (53/112, 47.3%) are enzymes. Of the 112 nonbinding to weakly binding proteins, 44 (39.3%) have previously been reported to react with autoantibodies. Strikingly, however, among the 63 proteins that were also present in DS-binding fractions, 50 (79.4%) are known autoantigens, corresponding to a more than twofold relative increase in autoantigenic propensity over the nonbinding to weakly binding group.

A total of 232 DS-binding proteins (eluting with 0.4, 0.6, or 1.0 mol/L NaCl) were identified (Table 2; see also Supplemental Appendix and references therein at *http://ajp.amjpathol.org*). Among them, 140 (60.3%) proteins have been previously described as autoantigens (Table 2; see also Supplemental Appendix and references therein at *http://ajp.amjpathol.org*). Remarkably, these DS-binding proteins cluster into several well-known categories of autoantigens,[2] including 40 chromatin-related proteins, 68 ribonucleoproteins or ribosomal proteins, 29 cytoskeletal proteins, 11 heat shock proteins, 27 en-

zymes, 30 protein processing-related proteins, 4 nucleolar phosphoproteins, and 4 nuclear pore complex proteins. In general, proteins with the strongest affinity to DS were histones, ribosomal proteins, heat shock proteins, and cytoskeletal proteins, whereas enzymes and protein processing-related proteins possessed lower affinity to DS (Table 2; see also Supplemental Appendix and references therein and Supplemental Table S3 at *http://ajp.amjpathol.org*).

Well-known autoantigenic nuclear proteins, such as histones, Scl-70, PCNA, Ro, La, and Ku, were present predominantly in the DS-binding fractions (0.4 mol/L to 1.0 mol/L elutions) (Table 2 and Figure 1; see also Supplemental Appendix and references therein and Supplemental Figure S1 at *http://ajp.amjpathol.org*). With the exception of histones, none of these were identified in either total unfractionated proteins (see Supplemental Table S2 at *http://ajp.amjpathol.org*) or the 0.2 mol/L fraction (see Supplemental Table S3 at *http://ajp.amjpathol.org*). Also prominently represented in DS-binding fraction was a large group of ribonucleoproteins, proteins related to the ribosome (including components of the large and small ribosomal subunits) and nucleolar proteins such as nucleolin (Table 2; see also Supplemental Appendix and references therein at *http://ajp.amjpathol.org*). In fact, these proteins were among the most abundant proteins extracted from WIL2-NS cells (see Supplemental Table S2 at *http://ajp.amjpathol.org*) and also highly abundant in DS-binding fractions. In particular, the Sm autoantigens (small nuclear ribonucleoproteins) were identified only in DS-binding fractions (Table 2; see also Supplemental Appendix and references therein at *http://ajp.amjpathol.org*), not in nonbinding or weakly binding fractions. Affinity to DS characterizes at least seven Sm autoantigens, including U2 snRNP-A′, U2 snRNP-B″, and Sm D2.

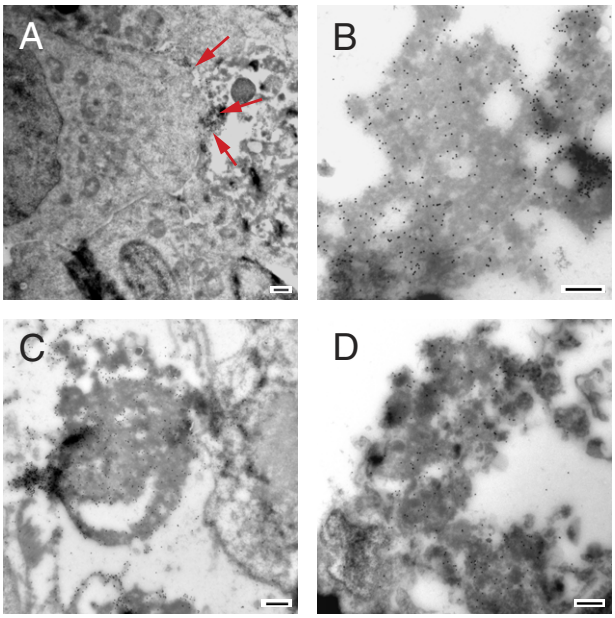

Figure 3. Direct association of DS with dead WIL2-NS cells. WIL2-NS cells were cultured with DS-biotin for 1 day to 3 days, and frozen sections of cells were labeled with anti-biotin gold particle conjugates (diameter, 20 nm) for examination by electron microscopy. **A:** DS (small dots) associated with dead cell debris (**arrows**) just outside a viable cell (visible to the **left**). **B:** Higher magnification showing DS association with cell debris. **C:** DS associated with fibrillar membrane-type cell debris. **D:** DS associated with dead cell blebs. Note part of a dead cell nucleus (**left bottom corner**). Scale bar = 500 nm (all panels).

Discussion

Here and in our companion article,[11] we provide experimental support for the hypothesis that complexation of a self-molecule with the glycosaminoglycan DS promotes specific B-1a cell responses and autoantibody production, thus rendering the self-molecule autoantigenic. Using proteome fractionation as a physicochemical selection mechanism for interrogating affinity to DS, we identified 246 distinct proteins (eluting at ≥0.4 mol/L NaCl; Tables 1 and 2; see also Supplemental Appendix and references therein at *http://ajp.amjpathol.org*), of which at least 147 (59.8%) are previously well-known autoantigens or closely related to known autoantigens. It is likely that the remaining proteins contain additional autoantigens yet to be recognized as such. If weakly DS-binding proteins are included (ie, eluting at 0.2 mol/L NaCl; see also Supplemental Table S3 at *http://ajp.amjpathol.org*), the above numbers become 357 (DS-binding proteins) and 191 (known autoantigens), respectively. It has been estimated that the autoantigen-ome represents ~1% of all human proteins (ie, approximately 200 to 300 individual autoantigens).[2] This means that physicochemical association with DS may capture virtually the entire autoantigen-ome in a single step.

We first tested this hypothesis focusing on well-characterized ANA/ENA autoantigens (Figure 1; see also Supplemental Figure S1 at *http://ajp.amjpathol.org*). All tested ANA and ENA autoantigens were enriched in DS-binding fractions, and some, such as PCNA, were detectable only after DS-affinity enrichment. We then investigated the utility of DS-affinity enrichment for the characterization of autoantigen repertoires in human autoimmune disease (Figure 2; see also Supplemental Figure S3 at *http://ajp.amjpathol.org*). The experiments revealed the clinical presence of autoantibodies to many more autoantigens than previously thought and conventionally assayed for. Autoimmune diseases remain among the most poorly defined medical conditions. Both the complexity and the diversity of the patient-specific autoantigen profiles further attest to the challenge of precisely classifying these diseases, even in those that are traditionally considered one clinical entity, such as SLE. In fact, it seems attractive to envision both personalized classification and management of autoimmune conditions based on comprehensive autoantibody/autoantigen profiling and time-course evolution.

We next attempted to comprehensively characterize the set of all autoantigens with affinity to DS. The 46 proteins identified by sequencing of selected bands or spots from 1-D and 2-D gels proved to be either known autoantigens or closely associated with autoimmunity (Table 1; see also Supplemental Appendix and references therein at *http://ajp.amjpathol.org*). Extension to un-

biased mass spectrometric shotgun sequencing identified a set of >200 proteins that are dominated by autoantigens (Table 2; see also Supplemental Appendix and references therein at *http://ajp.amjpathol.org*). Notably, the autoantigen-ome comprising approximately 200 autoantigens identified by DS-affinity fractionation is highly consistent with the estimated total human autoantigen repertoire.[2] All major classes of autoantigens, such as ANA, ENA, cytoskeletal components, and heat shock proteins, were identified.

A significant portion of DS-binding (especially tightly binding) proteins are components of chromatin or ribonucleoproteins (ie, molecules associated with DNA or RNA). DS resembles DNA and RNA, in that all three are densely anionic polymers. From this, one may speculate that DS can compete with DNA or RNA and become associated with proteins via their DNA- or RNA-binding surfaces. Furthermore, it is possible that DS can bind autoantigens at other sites as well. For example, we found evidence that Scl-70 can bind DS and DNA simultaneously in a ternary complex (Figure 1B). If autoantigens are binding partners for polyionic molecules, it might explain why autoantigens frequently possess long chains of charged residues.[9]

Another class of autoantigens identified in this study consists of components of the cytoskeleton, including actin, vimentin, tubulin, spectrin, and actinin. Autoantibodies to the cytoskeleton, targeting microtubules, microfilaments, or intermediate filaments, have been found in a diverse spectrum of diseases.[2] Glycosaminoglycans are known to be a major component of extracellular matrices, and it will be interesting to investigate whether DS and/or other glycosaminoglycans can associate intracellularly with the cytoskeleton or nuclear matrix, depending on physiological or pathogenic stimuli.

Although in the present study we focused on DS-binding autoantigen identification from affinity fractionated proteomes, autoantigens may not necessarily be in direct physical contact with DS. They may bind to DS directly or indirectly via one or more DS-binding scaffold molecules in a multimolecular complex. We speculate that some of the proteins eluted with lower concentrations of NaCl (eg, 0.2 mol/L) could be associated with DS via a protein that is eluted at higher salt concentration (eg, 1.0 mol/L). Although tightly DS-binding proteins are primarily chromatin-related proteins, ribonucleoproteins, or cytoskeletal proteins, those with lower DS affinity contain a set of enzymes that may in turn be associated with proteins that are tightly associated with DS.

With respect to the pathophysiologic role of DS•autoantigen association, we show in the companion article that DS preferentially associates with dead or apoptotic cells in murine models.[11] This also holds for human WIL2-NS cells (Figure 3). As shown by electron microscopy, DS preferentially associates with dead cells or cell debris, supporting the notion that dead cells serve as a source of autoantigens.[6,11]

In the companion study, we further show in both cell culture and in mice that DS•antigen complexes promote robust Ig responses to an antigen but not to DS.[11] To test whether this is also the case in humans, we measured DS-specific IgG and IgM in patient sera. Indeed, all patients had very low levels of IgM or IgG against DS (see Supplemental Figure S6 at *http://ajp.amjpathol.org*). Total IgM ranged from 0.3 mg/mL to 2.8 mg/mL, whereas DS-specific IgM ranged from 0.2 μg/mL to 3.4 μg/mL, accounting for approximately 0.1% of total IgM (see Supplemental Figure S6A at *http://ajp.amjpathol.org*). Similarly, total IgG ranged from 7 mg/mL to 42 mg/mL, whereas DS-specific IgG ranged from 0.4 μg/mL to 1.9 μg/mL, accounting for <0.05% of total IgG (see Supplemental Figure S6B at *http://ajp.amjpathol.org*).

Abnormal glycosaminoglycan metabolism has been observed in numerous autoimmune conditions.[19,20] It is possible that DS production is increased during high cell turnover (eg, increased cell apoptosis in SLE) or with increased cell regeneration, turnover, and dead cell removal during wound healing. DS shares structural similarities with other endogenous and exogenous glycosaminoglycans, including heparin, heparan sulfate, and hyaluronic acid. DS also shares structural features with dextran sulfate, a known B cell mitogen.[21] Furthermore, as a member of the polysaccharide family, DS mimics in various structural aspects polysaccharides that are expressed abundantly on the cell surfaces of microbial pathogens.[22] Is it therefore possible that autoimmune diseases can be triggered by microbial infections through interaction of host molecules with microbial polysaccharides.

In sum, the present findings suggest affinity to DS as a unifying physicochemical property of human autoantigens and as a powerful and novel approach for the enrichment, identification, and near-complete characterization of the entire human autoantigen-ome, thus providing a promising method for the molecular stratification of clinically similar autoimmune diseases.

Acknowledgments

We thank Jongmin Lee, Ph.D., Ming Yan, Ph.D., Serena Leone, Ph.D., and Sidney Wang, Ph.D. (all at Harvard Medical School), for insightful discussions. We thank Ross Tomaino, Ph.D., and Steven Gygi, Ph.D., (Taplin Biological Mass Spectrometry Facility, Harvard Medical School) and Maria Ericsson (electron microscopy facility, Harvard Medical School) for expert assistance.

References

1. Plotz PH: The autoantibody repertoire: searching for order. Nat Rev Immunol 2003, 3:73–78
2. Amital H, Shoenfeld Y: Natural autoantibodies, heralding, protecting and inducing autoimmunity. Autoantibodies, ed 2. Edited by Y Shoenfeld, ME Gershwin, PL Meroni. Amsterdam, Elsevier, 2007, pp 7–12
3. Gilbert D, Brard F, Jovelin F, Tron F: Do naturally occurring autoantibodies participate in the constitution of the pathological B-cell repertoire in systemic lupus erythematosus? J Autoimmun 1996, 9:247–257
4. Fairweather D, Frisancho-Kiss S, Rose NR: Sex differences in autoimmune disease from a pathological perspective. Am J Pathol 2008, 173:600–609
5. Cohen PL, Maldonado MA: Animal models for SLE. Curr Protoc Immunol 2003, Chapter 15:Unit 15.20

6. Casciola-Rosen L, Andrade F, Ulanet D, Wong WB, Rosen A: Cleavage by granzyme B is strongly predictive of autoantigen status: implications for initiation of autoimmunity. J Exp Med 1999, 190:815–826
7. Fourneau JM, Bach JM, van Endert PM, Bach JF: The elusive case for a role of mimicry in autoimmune diseases. Mol Immunol 2004, 40: 1095–1102
8. Powell AM, Black MM: Epitope spreading: protection from pathogens, but propagation of autoimmunity? Clin Exp Dermatol 2001, 26:427–433
9. Dohlman JG, Lupas A, Carson M: Long charge-rich alpha-helices in systemic autoantigens. Biochem Biophys Res Commun 1993, 195: 686–696
10. Nozawa K, Fritzler MJ, Chan EK: Unique and shared features of Golgi complex autoantigens. Autoimmun Rev 2005, 4:35–41
11. Wang JY, Lee J, Yan M, Rho J, Roehrl MHA: Dermatan sulfate interacts with dead cells and regulates $CD5^+$ B-cell fate: implication for a key role in autoimmunity. Am J Pathol 2011, 178:2168–2176
12. Shevchenko A, Wilm M, Vorm O, Mann M: Mass spectrometric sequencing of proteins silver-stained polyacrylamide gels. Anal Chem 1996, 68:850–858
13. Peng J, Gygi SP: Proteomics: the move to mixtures. J Mass Spectrom 2001, 36:1083–1091
14. Damoiseaux JG, Tervaert JW: From ANA to ENA: how to proceed? Autoimmun Rev 2006, 5:10–17
15. Nojima J, Iwatani Y, Ichihara K, Tsuneoka H, Ishikawa T, Yanagihara M, Takano T, Hidaka Y: Acquired activated protein C resistance is associated with IgG antibodies to protein S in patients with systemic lupus erythematosus. Thromb Res 2009, 124:127–131
16. Lu J, Willis AC, Sim RB: A calreticulin-like protein co-purifies with a '60 kD' component of Ro/SSA, but is not recognized by antibodies in Sjögren's syndrome sera. Clin Exp Immunol 1993, 94: 429–434
17. McCauliffe DP, Yang YS, Wilson J, Sontheimer RD, Capra JD: The 5′-flanking region of the human calreticulin gene shares homology with the human GRP78, GRP94, and protein disulfide isomerase promoters. J Biol Chem 1992, 267:2557–2562
18. Chan EK, Sullivan KF, Tan EM: Ribonucleoprotein SS-B/La belongs to a protein family with consensus sequences for RNA-binding. Nucleic Acids Res 1989, 17:2233–2244
19. Edward M, Fitzgerald L, Thind C, Leman J, Burden AD: Cutaneous mucinosis associated with dermatomyositis and nephrogenic fibrosing dermopathy: fibroblast hyaluronan synthesis and the effect of patient serum. Br J Dermatol 2007, 156:473–479
20. Parildar Z, Uslu R, Tanyalcin T, Doganavsargil E, Kutay F: The urinary excretion of glycosaminoglycans and heparan sulphate in lupus nephritis. Clin Rheumatol 2002, 21:284–288
21. Aoyama E, Yoshihara R, Tai A, Yamamoto I, Gohda E: PKC- and PI3K-dependent but ERK-independent proliferation of murine splenic B cells stimulated by chondroitin sulfate B. Immunol Lett 2005, 99: 80–84
22. Choi YH, Roehrl MH, Kasper DL, Wang JY: A unique structural pattern shared by T-cell-activating and abscess-regulating zwitterionic polysaccharides. Biochemistry 2002, 41:15144–15151